

A 0.31THz CMOS Uniform Circular Antenna Array Enabling Generation/Detection of Waves with Orbital-Angular Momentum

Muhammad Ibrahim Wasiq Khan¹, Jongchan Woo¹, Xiang Yi^{1,2}, Mohamed I. Ibrahim¹,
Rabia Tugce Yazicigil³, Anantha Chandrakasan¹, Ruonan Han¹

¹Massachusetts Institute of Technology, Cambridge MA USA

²South China University of Technology, Guangzhou China

³Boston University, Boston MA USA

Abstract—This paper reports the first chip-based demonstration (at any frequency) of a CMOS front-end that generates and receives electromagnetic waves with rotating wave phase front (namely orbital angular momentum or OAM). The chip, based on a uniform circularly placed patch antenna array at 0.31THz, transmits reconfigurable OAM modes, which are digitally switched among the $m=0$ (plane wave), $+1$ (left-handed), -1 (right-handed) and superposition $(+1)+(-1)$ states. The chip is also reconfigurable into a receiver mode that identifies different OAM modes with $>10\text{dB}$ rejection of unintended modes. The array, driven by only one active path, has a measured EIRP of -4.8dBm and consumes 154mW of DC power in the OAM source mode. In the receiver mode, it has a measured conversion loss of 30dB and consumes 166mW of DC power. The output OAM beam profiles and mode orthogonality are experimentally verified and a full silicon OAM link is demonstrated.

Keywords—Terahertz, orbital angular momentum, OAM modes, uniform circular antenna array, orthogonal, multiplier-amplifier chain.

I. INTRODUCTION

Multiplexing of electromagnetic (EM) waves with different frequencies, polarizations and coding has been extensively exploited in wireless systems. Recently, another dimension of EM wave - the orbital angular momentum (OAM), is attracting increasing attentions [1]. An OAM-based wave possesses a wavefront with a helical phase distribution around the central axis of the beam. Different OAM modes, determined by the handedness and the total phase change ($\phi = 2m\pi$, $m = 0, \pm 1, \pm 2, \dots$) of the wavefront twist, are orthogonal. Previously, multi-OAM-mode transmission has been studied for the enhancement of spectrum efficiency [1]–[4]. Another attractive application of OAM wireless system is the physical-layer security in the one-way transmission of secret key for symmetric encryption (e.g. AES), which relies on trustworthy key distribution. Traditional wireless transmission is susceptible to eavesdropping at unintended positions, due to beam divergence and antenna sidelobes. In comparison, the instantaneous mode of an OAM beam when driven by the bits of the secret key, the mode information lies within the phase twist around the beam axis (Fig. 1). It can only be effectively detected by a receiver with multiple phase-comparing antennas located around that axis. Such positioning requirement boosts the robustness against eavesdropping at off-axis locations [5], [6], where the SNR of the inter-antenna phase gradient rapidly drops below the detectable threshold.

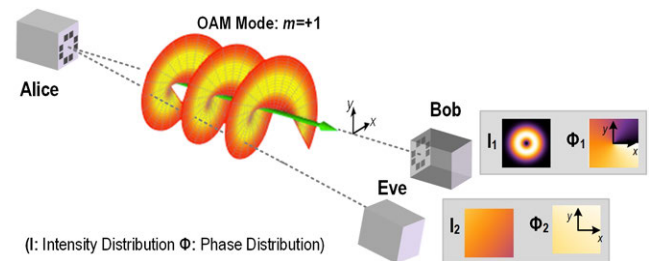


Fig. 1. Potential application of OAM generator/receptor in physically-secure wireless link against off-beam-axis eavesdropping

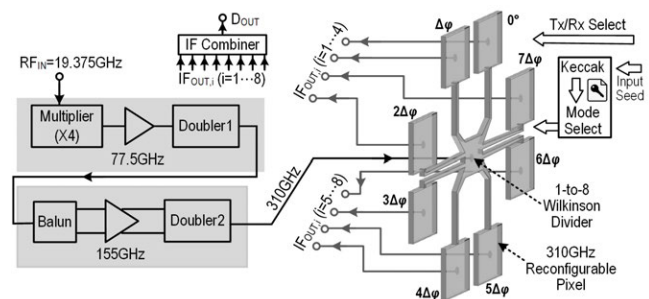
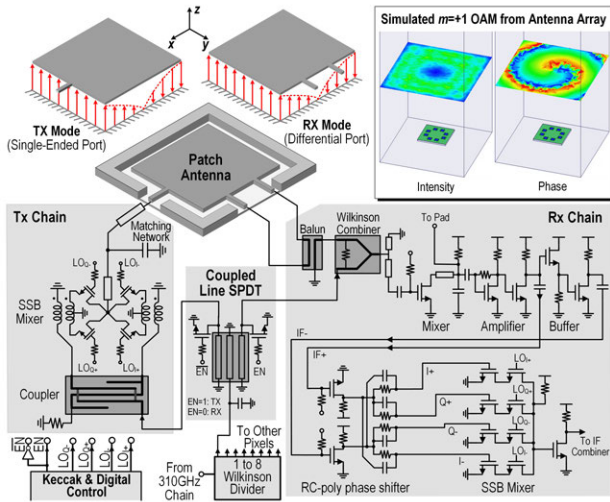


Fig. 2. The architecture of the THz chip for OAM generation/reception

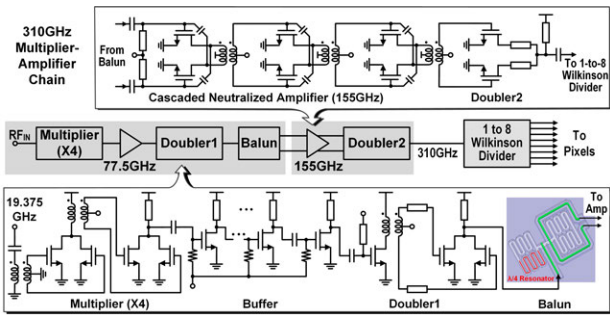
Conventional OAM-generation approaches incorporate dielectric spiral-phase plate, passive uniform circular antenna array or metasurface in conjunction with separate signal drivers [1]–[4]. These discrete solutions, however, lead to very bulky and costly systems. Up till now, no chip-based OAM component at any frequency is reported. In this paper, we for the first time present a CMOS active antenna array that can not only generate/receive OAM waves at 310GHz , but also perform electrical OAM mode switching among the $m=+1$ (left-handed), -1 (right-handed), $(+1)+(-1)$ (superposition) and $m=0$ (plane wave) states. The above multiplexing and security applications are therefore made possible at the chip scale.

II. ARCHITECTURE AND CIRCUIT DESIGN DETAILS

The chip architecture, shown in Fig. 2, consists of eight reconfigurable THz modulator/detector units (referred as pixel henceforth) driven by a 310GHz signal generator through a 1-to-8 Wilkinson divider. The pixels with their integrated patch antennas are placed in a uniform circular pattern with a diameter of about one wavelength in free space. In the OAM



(a)



(b)

Fig. 3. Schematics of (a) the 310GHz OAM pixel, and (b) the 310GHz multiplier-amplifier chain.

transmission mode, each pixel generates radiation with a phase difference of $\Delta\phi$ with respect to its neighbouring pixels. $\Delta\phi$ values of 0 , $+45^\circ$, -45° therefore correspond to the OAM modes of $m=0$, $+1$ (simulated in Fig. 3a) and -1 , respectively. An on-chip Keccak block generates data of a random key, which can be mapped to the instantaneous OAM modes for transmission. In the reception mode, each pixel mixes its received wave with the local 310GHz signal and generates an IF output. An analog phase comparator of these IF signals enables the determination of the incident OAM mode.

A. Design of Antenna-Integrated THz Pixel

The schematic of the THz OAM pixel is shown in Fig. 3a. The Tx/Rx mode selection is realized by a coupled-line-based SPDT switch [7], which directs the 310GHz input to either a Tx chain or a Rx chain. The simulated insertion loss and isolation of the switch are 3.8dB and 15dB, respectively. In the Tx chain, the aforementioned phase shifting is implemented through a single-sideband (SSB) mixer, which is driven by a quadrature 8MHz LO from the on-chip digital controller. Through the selection of LO phases, the controller changes the THz output phase, generating different OAM modes from the array. Compared to conventional high-frequency phase shifters, our mixer-based scheme offers precise phase control

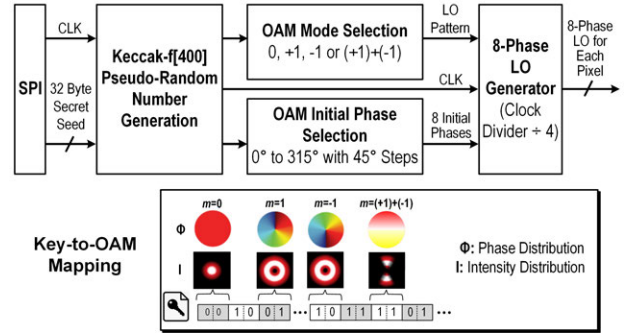


Fig. 4. On-Chip secret key generator and OAM-mode controller with key-to-OAM mapping

and phase-independent amplitude response, which are critical to the fidelity of OAM wavefront. Mode switching is realized by the data-driven selection of the LO phases. The mode switching speed, although limited by the LO frequency, is sufficient for the transmission of secret key (typically 256 bit). In simulation, $\sim 8\mu\text{W}$ of 310GHz power is radiated from the single-ended patch antennas.

For chip compactness, the receiver mode uses the same antenna, where the input wave is extracted through a differential feeds along the antenna H-plane (Fig. 3a). The SPDT-directed 310GHz signal, which combines with the received signal in a Wilkinson combiner, behaves as a THz LO that down-converts the received signal inside a MOSFET-based square-law mixer. The generated IF signal, carrying the same phase as the local input wave, is then amplified and undergoes a phase shifting process inside a SSB mixer (for the same reason as that in generation mode). When such a phase shift compensates the OAM phase gradient $\Delta\phi$ among the THz pixels, all IF outputs become in-phase. The IF combiner in Fig. 2 then adds them constructively and provides D_{OUT} as an indicator of whether the incident wave matches the currently selected OAM mode. For simultaneous detection of multiple OAM modes, the pixel IF signals can be directly extracted through pads and independently processed off chip.

B. 310GHz Multiplier-Amplifier Chain and Data Controller

In Fig. 3b, the 310 GHz multiplier-amplifier signal source is shown. A 19.375 GHz input signal is frequency quadrupled and then doubled. Through a folded slot balun, it then drives a chain of cascaded pseudo-differential 155GHz amplifiers that are based on transformer coupling and neutralization. Finally, a second doubler with a saturated input power of 0dBm is deployed to generate the 310GHz signal.

A Keccak-f[400] block supporting absorb and squeeze for sponge construction is used as a source of raw entropy to generate 256 random bits at a clock frequency of 32MHz (Fig. 4). Through the selection from eight available LO phase patterns for each THz pixel, every two bits of the Keccak random output are converted to an OAM mode with a mapping table shown in Fig. 4. The eight-phase LO signals at 8MHz are generated by a divider ($\div 4$) driven by the input clock.

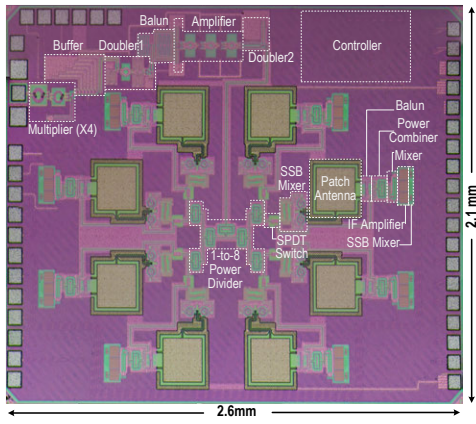


Fig. 5. Die photo of the 310GHz OAM CMOS chip.

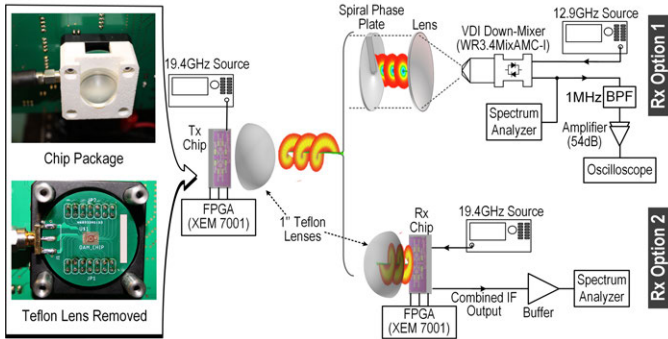


Fig. 6. The measurement setup for the CMOS chip.

III. MEASUREMENT RESULTS

Fabricated in a 65nm CMOS process, the chip occupies $2.6 \times 2.1 \text{mm}^2$ area (Fig. 5). The measurement setup is shown in Fig. 6. Given the relatively large divergence of OAM beam, a one-inch Teflon lens is included in the chip package to collimate the beam. First, the radiated power of OAM array is measured by configuring the chip to generate plane wave ($m=0$ mode), and by placing a calibrated VDI WR-3.4 sub-harmonic mixer with a feedhorn (26dBi gain) 25cm away; the corresponding measured EIRP of the chip is -4.8dBm . Next, the VDI receiver is mechanically scanned across a 2D plane facing the chip, in order to measure the wavefront intensity distribution of the chip output. The results in Fig. 7 show the expected null at the center of the $m=+1$ OAM mode. Our chip also enables and utilizes the superposition of the $m=+1$ and -1 modes, and the measured plot in Fig. 7 presents the expected standing peaks and nulls as the result of the summation of the two counter-rotating wavefronts.

A direct measurement of phase distribution is challenging, due to the required μm -level Rx position precision at THz frequency; instead, the setup shown in Fig. 6 (Rx Option 1) is adopted, where a set of 3D printed THz spiral phase plates (SPPs) are placed in front of the VDI receiver, and serve as “mode filters” by converting the input with matched OAM mode into a plane wave. The SPP has a measured loss of 12dB. For different combinations between OAM modes of the

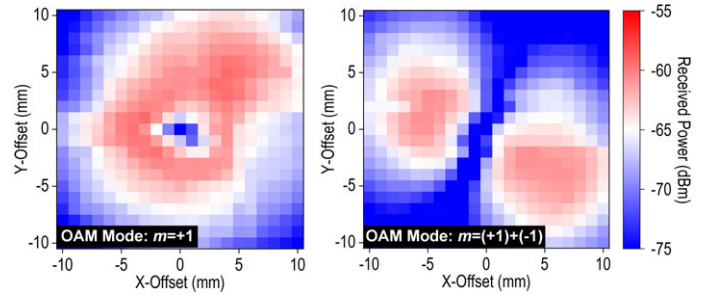


Fig. 7. Measured intensity distribution for OAM modes of $m=+1$ and $m=(+1)+(-1)$ (superposition) generated by the chip

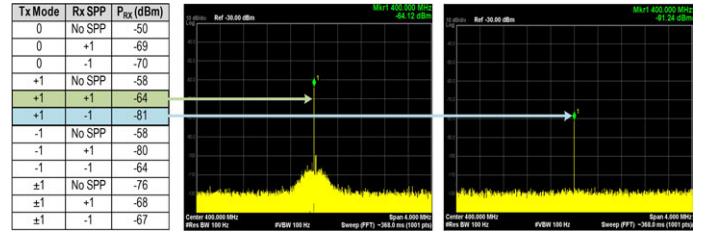


Fig. 8. OAM mode-checking using Option 1 Rx setup in Fig. 6. Note: when the Rx has no SPP and when the Tx mode is $m \neq 0$, ideally the Rx output power should be zero, but any off-axis misalignment of OAM array will get the Rx antenna to point at a non-zero portion of the OAM wavefront, resulting in non-negligible received power.

generating array and the configuration of Rx SPP ($m=+1$ or -1), the VDI receiver output power and spectrum are recorded in Fig. 8, showing 17dB difference between the matched and unmatched cases. Next, the OAM chip output mapped from a repeated 1Mbps Keccak-generated data sequence is verified, and the time-domain outputs of the Rx with different SPP configurations are shown in Fig. 9, which shows good correlation with matched modes, partial correlation of $m=+1$ or $m=-1$ mode with superposition $m=(+1)+(-1)$ mode, as well as rejection of unmatched modes.

To test the reception mode of the chip, a VDI WR3.4 source ($P_{out} = -5 \text{dBm}$) is used. The measured conversion loss of the chip for plane wave ($m=0$) $\sim 30 \text{dB}$. Next, with a SPP inserted (Fig. 10), the setup becomes an OAM mode generator. The chip shows $>10 \text{dB}$ rejection when the OAM modes on the two sides are unmatched for all combinations of OAM modes.

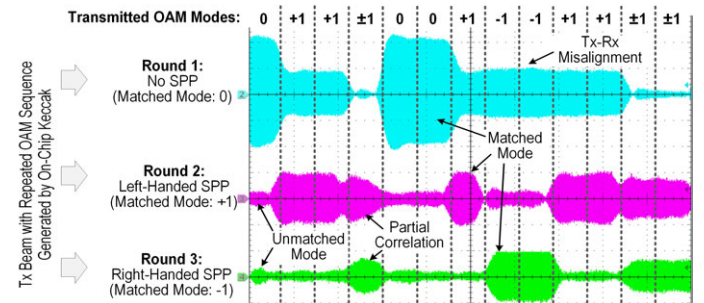


Fig. 9. Time-domain output of the receiver configured to respond to different OAM modes, when it is illuminated by the same OAM sequence generated by on-chip Keccak

Table 1. Comparison with Prior RF and mm-Wave OAM Prototypes based on discrete components

	[2]	[3]	[4]	This work
Implementation	Discrete Transceivers +SPP+Quasi-Optical Beam Combiner	Active-Driven Antenna Arrays+Parabolic Reflectors	Active-Driven Antenna Arrays	Active-Driven Antenna Array on a 65nm CMOS Chip+Teflon Lens
Frequency (GHz)	28	10	40	310
OAM Modes	$\pm 1, \pm 3$	$\pm 2, \pm 3$	$0, \pm 1, \pm 2, \pm 3$	$0, +1, -1, \pm 1$
Data Modulation	16QAM/Mode Dual Polarization	32QAM on each mode, Full Duplex	256QAM/Mode Dual Polarization	Bit-to-Mode OAM Hopping
Radiated Power (dBm)	8	0	11.5	-4.8 (EIRP)
Antenna Aperture Diameter (cm)	30	60	120	1.35
Application	Enhanced Spectral Efficiency	Enhanced Spectral Efficiency	Enhanced Spectral Efficiency	Physical-Layer Security
DC Power (mW)	N/A	N/A	N/A	154 (Tx) 166 (Rx)

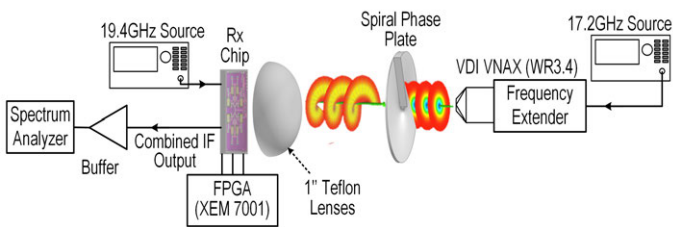


Fig. 10. The experimental setup for receive mode characterization

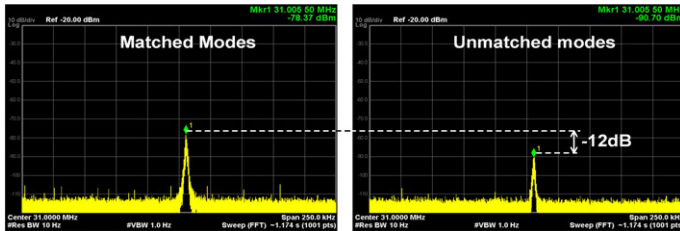


Fig. 11. Measured spectrum of combined IF in Rx mode when modes are matched and unmatched

One example is shown in Fig. 11: the VDI Tx is always in $m=+1$ mode, while the chip detection mode is configured to $m=+1$ and $m=-1$, respectively.

Finally, a full-silicon OAM link is tested using the Option 2 in Fig. 6. When the two chips are configured to be the $m=+1$ mode, an Rx IF output that is highly sensitive to the Rx offset from the array axis, is obtained (Fig. 12). That demonstrates the aforementioned physical-layer security.

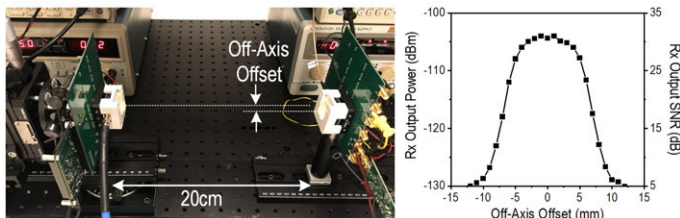


Fig. 12. Full-silicon OAM link and sensitivity to co-axial alignment

IV. CONCLUSION

A 0.31THz uniform circular patch antenna array is demonstrated in 65nm CMOS process that can generate and receive waves carrying orbital angular momentum. The chip dynamically generates data-driven OAM modes: $m=0, +1, -1$ and $(+1)+(-1)$ as well as detect these mode with >10 dB rejection of unintended modes. Table 1 provides a comparison with other discrete-component-based OAM prototypes. Our work is the first demonstration of full-silicon OAM link at any frequency, as well as the first hardware delivering reconfigurable OAM modes in the THz regime. It opens up the opportunities in the enhancement of wireless spectral efficiency and physical-layer-security of key transmission using low cost microelectronic chips.

ACKNOWLEDGMENT

The authors thank NSF for the funding from an EAGER SARE award and Prof. Yang Yang at University of Technology, Sydney for the SPP plates.

REFERENCES

- [1] W. Cheng, W. Zhang, H. Jing, S. Gao, and H. Zhang, "Orbital Angular Momentum for Wireless Communications," *IEEE Wireless Communications*, vol. 26, no. 1, pp. 100–107, Feb. 2019.
- [2] Y. Yan, X. Guodong, L. Martin P. J., H. Hao, A. Nisar, B. Changjing, R. Yongxiong, C. Yinwen, L. Long, Z. Zhe, M. A. T. Moshe, P. Miles J., and W. Alan E., "High-capacity millimetre-wave communications with orbital angular momentum multiplexing," *Nature Comm.*, Sep. 2014.
- [3] W. Zhang, S. Zheng, X. Hui, R. Dong, X. Jin, H. Chi, and X. Zhang, "Mode division multiplexing communication using microwave orbital angular momentum: An experimental study," *IEEE Transactions on Wireless Communications*, vol. 16, no. 2, pp. 1308–1318, 2017.
- [4] H. Sasaki, Y. Yagi, T. Yamada, T. Semoto, and D. Lee, "An experimental demonstration of over 100 Gbit/s OAM multiplexing transmission at a distance of 100 m on 40 GHz band," in *2020 IEEE International Conference on Communications Workshops*, 2020, pp. 1–6.
- [5] W. Huang, Y. Li, D. Wei, and Q. Zhang, "Research on physical layer security scheme based on OAM," vol. 11604, Jun. 2019, p. 573–586.
- [6] I. B. Djordjevic, "OAM-Based Hybrid Free-Space Optical-Terahertz Multidimensional Coded Modulation and Physical-Layer Security," *IEEE Photonics Journal*, vol. 9, no. 4, pp. 1–12, 2017.
- [7] F. Meng, K. Ma, K. S. Yeo, C. C. Boon, W. M. Lim, and S. Xu, "A 220–285 GHz SPDT switch in 65-nm cmos using switchable resonator concept," *IEEE Transactions on Terahertz Science and Technology*, vol. 5, no. 4, pp. 649–651, 2015.